CHEMISTRY
A EUROPEAN JOURNAL

ChemPubSoc Europe

DOI: 10.1002/chem.201200597

Environment-Sensitive Fluorophores with Benzothiadiazole and Benzoselenadiazole Structures as Candidate Components of a Fluorescent Polymeric Thermometer

Seiichi Uchiyama,*[a] Kohki Kimura,[b] Chie Gota,[a] Kohki Okabe,[a] Kyoko Kawamoto,[a] Noriko Inada,[c] Toshitada Yoshihara,[b] and Seiji Tobita*[b]

Abstract: An environment-sensitive fluorophore can change its maximum emission wavelength (λ_{em}), fluorescence quantum yield (Φ_f), and fluorescence lifetime in response to the surrounding environment. We have developed two new intramolecular charge-transfer-type environment-sensitive fluorophores, DBThD-IA and DBSeD-IA, in which the oxygen atom of a well-established 2,1,3-benzoxadiazole environment-sensitive fluorophore, DBD-IA, has been replaced by a sulfur and selenium atom, respectively. DBThD-IA is highly fluorescent in *n*-hexane ($\Phi_f = 0.81$, $\lambda_{em} = 537$ nm) with excitation at 449 nm, but is almost non-fluorescent in water ($\Phi_f = 0.037$, $\lambda_{em} = 616$ nm), similarly to DBD-IA ($\Phi_f = 0.91$, $\lambda_{em} = 520$ nm in *n*-hexane; $\Phi_f = 0.027$, $\lambda_{em} = 616$ nm in water). A similar variation in fluorescence properties was also observed for DBSeD-IA ($\Phi_f = 0.24$, $\lambda_{em} = 591$ nm in *n*-hexane; $\Phi_f = 0.0046$, $\lambda_{em} = 672$ nm in water). An intensive study of the solvent effects on the fluorescence properties of these fluorophores revealed that both the polarity of the environment and hydrogen bonding with solvent molecules accelerate the nonradiative relaxation of the excited fluorophores. Time-resolved optoacoustic and phosphorescence measurements clarified that both intersystem crossing and internal conversion are involved in the nonradiative relaxation processes of DBThD-IA and DBSeD-IA. In addition, DBThD-IA exhibits a 10-fold higher photostability in aqueous solution than the original fluorophore DBD-IA, which allowed us to create a new robust molecular nanogel thermometer for intracellular thermometry.

Keywords: chromophores · fluorescence · photochemistry · photophysics · sensors

Introduction

Environment-sensitive fluorophores exhibit different fluorescence properties (e.g., maximum emission wavelength, fluorescence quantum yield, and fluorescence lifetime) depending on their surroundings. In previous studies, prodan,[1] ANS–Na,[2] dansylamine,[3] NBD-NHMe (nitrobenzofurazan),[4] and Nile red[5] (Figure 1, the chemical names are provided in the Experimental Section) were used as representative environment-sensitive fluorophores. Most conventional environment-sensitive fluorophores, including these representatives, exhibit weaker emission at longer wavelengths in more polar and protic environments, but a few examples display different behavior.[6] Thus, environment-sensitive fluorophores can be used for evaluating the microenvironment near a three-dimensional structure, such as a protein,[7] DNA,[8] micelle,[9] or silica.[10] In addition, the dynamic conformational changes of a protein that are induced by external stimuli (e.g., heat,[11] voltage,[12] or inhibitors[13]), protein–

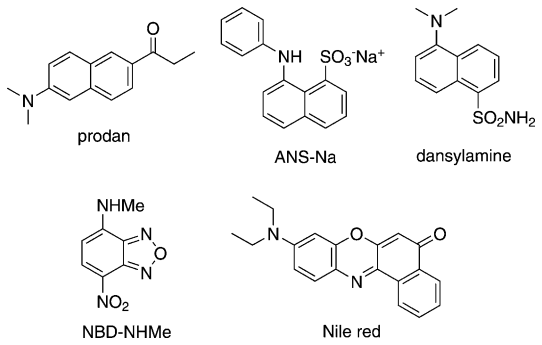

Figure 1. Chemical structures of representative examples of environment-sensitive fluorophores.

[a] Dr. S. Uchiyama, C. Gota, Dr. K. Okabe, K. Kawamoto
Graduate School of Pharmaceutical Sciences
The University of Tokyo
7-3-1 Hongo, Bunkyo-ku, Tokyo 113-0033 (Japan)
Fax: (+81) 3-58414768
E-mail: seiichi@mol.f.u-tokyo.ac.jp

[b] K. Kimura, Dr. T. Yoshihara, Prof. S. Tobita
Department of Chemistry and Chemical Biology
Graduate School of Engineering, Gunma University
1-5-1 Tenjin-cho, Kiryu, Gunma 376-8515 (Japan)
Fax: (+81) 277-30-1213
E-mail: tobita@gunma-u.ac.jp

[c] Dr. N. Inada
Graduate School of Biological Sciences
Nara Institute of Science and Technology
8916-5 Takayama-cho, Ikoma, Nara 630-0192 (Japan)

Supporting information for this article is available on the WWW under http://dx.doi.org/10.1002/chem.201200597.

protein[14] (or protein–peptide[15]) interactions, and the insertion of a protein into a cell membrane[16] can also be monitored by using environment-sensitive fluorophores.[17]

Recently, another use for environment-sensitive fluorophores was reported for new fluorescent sensing systems[18–20] in which an environment-sensitive fluorophore is covalently attached to a stimulus-responsive macromolecule (e.g., protein, peptide, or synthetic polymer). In the pioneering work reported by Walkup and Imperiali,[21] a zinc-binding peptide labeled with dansylamine functioned as a fluorescent zinc ion sensor: The environment-sensitive fluorophore transformed the microenvironmental change induced by the binding event between the peptide and the zinc ion into a fluorescence signal. Within a decade, this type of fluorescent sensor was intensively developed to target various ions (calcium,[22] copper,[23] lead,[24] sulfate,[25] and phosphate[26]) and small molecules (glucose,[27] maltose,[28] and glutamine[29]). A fluorescent macromolecular sensor for Pi (inorganic phosphate) has been used to study the kinetics of ATP and GTP hydrolysis.[30]

A substituted 2,1,3-benzoxadiazole (benzofurazan)[31] is one fluorophore that is very sensitive to changes in the polarity and the hydrogen-bonding ability of a solvent. Although NBD-NHMe[4b] (Figure 1) is a more common and readily available environment-sensitive fluorophore with a benzofurazan structure, we used DBD-IA[32] (Figure 2) as

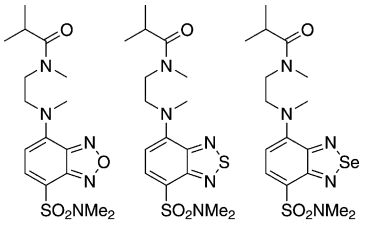

Figure 2. Chemical structures of DBD-IA, DBThD-IA, and DBSeD-IA.

a more sensitive fluorophore in previous studies for the development of thermoresponsive polymer-based fluorescent thermometers.[33] Owing to the high sensitivity of DBD-IA to its surroundings, a fluorescent polymeric thermometer composed of a thermoresponsive poly(*N*-isopropylacrylamide) unit (PNIPAM unit) and a DBD-IA unit emitted a 13.3-fold increase in fluorescence when the temperature of the aqueous solution increased from 29 to 37 °C. A very small change (0.3–0.5 °C) in the temperature inside living cells can be monitored by using a fluorescent polymeric thermometer created in the same manner.[34]

In this paper, we report on disubstituted benzothiadiazole and benzoselenadiazole derivatives (DBThD-IA and DBSeD-IA, shown in Figure 2) as new environment-sensitive fluorophores. The absorption and fluorescence spectra as well as the fluorescence lifetimes of the synthesized DBThD-IA and DBSeD-IA were measured in *n*-hexane, 1,4-dioxane, ethyl acetate, ethanol, 2,2,2-trifluoroethanol, methanol, [D_1]methanol (CH_3OD), acetonitrile, DMSO, water, and deuterium oxide to investigate the sensitivity of the fluorophores to variations in their environment. Readers can refer to our previous research in which the same set of solvents were used to investigate the photophysical properties of DBD-IA.[32] The fluorescence properties of DBThD-IA and DBSeD-IA in mixed solvents of 1,4-dioxane and water were also measured and compared with those of conventional environment-sensitive fluorophores. The photostabilities of DBThD-IA, DBSeD-IA, and DBD-IA were measured in selected nonaqueous and aqueous solvents because bioimaging with a fluorescence microscope is a potential application of these environment-sensitive fluorophores. In addition, time-resolved optoacoustic[35] and phosphorescence experiments were performed for DBThD-IA, DBSeD-IA, DBD-IA, and their derivatives sensitized by an iridium complex to determine the efficiencies of intersystem crossing and internal conversion in the relaxation processes.

Finally, one of the new fluorophores, DBThD-IA, was used as an environment-sensitive fluorophore to construct a fluorescent polymeric thermometer because it exhibits high photostability compared with DBD-IA used in previous studies.[32–34] A fluorescent monomer, DBThD-AA (Figure 3), and a fluorescent nanogel thermometer composed of DBThD-IA units were prepared. Studies on living cells revealed that this new fluorescent nanogel thermometer is remarkably resistant to photobleaching and therefore suitable for long-term monitoring of intracellular temperatures. Thus, DBThD-IA can replace DBD-IA, especially in cases in which the environment-sensitive-fluorophore-containing fluorescent macromolecular sensor has been designed for biological experiments accompanied by light irradiation.

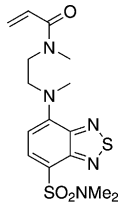

Figure 3. Chemical structure of a new environment-sensitive fluorescent monomer, DBThD-AA.

Results

Synthesis of DBThD-IA and DBSeD-IA: DBThD-IA and DBSeD-IA were synthesized according to Scheme 1. The 2,1,3-benzthiodiazole ring was obtained by the reaction between 1-chloro-2,3-diaminobenzene with *N*-thionylaniline, whereas the 2,1,3-benzoselenadiazole ring was constructed from the same diaminobenzene and selenium dioxide. A dimethylsulfamoyl group was introduced into the aromatic rings by using chlorosulfuric acid and an equimolar amount of dimethylamine. The chloro group was then replaced by an amino group by using *N*,*N*′-dimethylethylenediamine and subsequent acylation with isobutyric anhydride afforded DBThD-IA and DBSeD-IA.

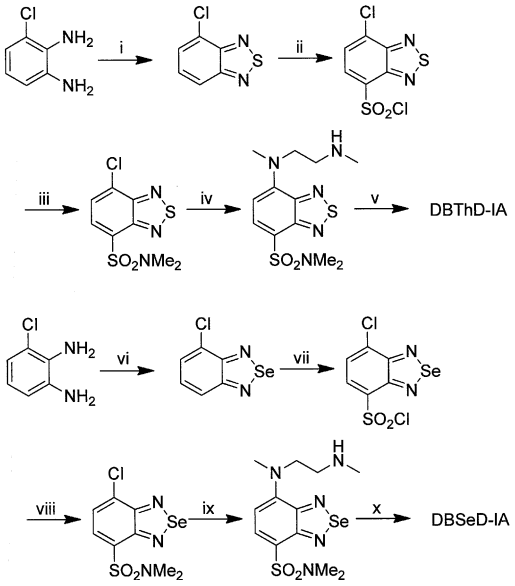

Scheme 1. Synthesis of DBThD-IA and DBSeD-IA. Reagents and conditions: i) PhNSO, toluene, reflux, 3 h (86%); ii) $ClSO_3H$, 0°C, 1.5 h→150°C, 2.5 h (79%); iii) Me_2NH, H_2O, MeCN, CH_2Cl_2, RT, 30 min (98%); iv) *N,N'*-dimethylethylenediamine, MeCN, 80°C, 1 h (>99%); v) isobutyric anhydride, TEA, MeCN, RT, 1 h (78%); vi) SeO_2, EtOH, 80°C, 30 min (99%); vii) $ClSO_3H$, 0°C, 1 h→150°C, 3 h (66%); viii) Me_2NH, H_2O, MeCN, CH_2Cl_2, RT, 30 min (85%); ix) *N,N'*-dimethylethylenediamine, MeCN, 80°C, 1 h (>99%); x) isobutyric anhydride, TEA, CH_2Cl_2, RT, 17 min (68%).

Absorption and fluorescence properties of DBThD-IA and DBSeD-IA: The absorption and fluorescence spectra of DBThD-IA and DBSeD-IA were recorded in 11 solvents of various polarities and hydrogen-bonding abilities, that is, *n*-hexane, 1,4-dioxane, ethyl acetate, ethanol, 2,2,2-trifluoroethanol, methanol, [D_1]methanol (CH_3OD), acetonitrile, DMSO, water, and deuterium oxide. Representative absorption and fluorescence spectra of DBThD-IA and DBSeD-IA are shown in Figure 4, and the maximum absorption wavelengths, molar absorption coefficients, maximum emission wavelengths, and fluorescence quantum yields are listed in Table 1. The fluorescence lifetimes of DBThD-IA and DBSeD-IA were measured in the same solvents. Representative fluorescence decay curves are also shown in Figure 4. Each fluorescence decay curve is well fitted by a single-exponential curve and the fluorescence lifetimes are listed in Table 1. The fluorescence and nonradiative rate constants were calculated and are also listed in Table 1. The results indicate that the fluorescence properties, that is, the maximum emission wavelengths, fluorescence quantum yields, and fluorescence lifetimes of DBThD-IA and DBSeD-IA are affected by the solvent, whereas the absorption properties, that is, the maximum absorption wavelengths and molar absorption coefficients, are relatively independent of solvent. In less polar or less protic solvents, the fluorescence quantum yields of both fluorophores are higher and their fluorescence lifetimes are longer. Comparison of the fluorescence properties of DBThD-IA and DBSeD-IA in the same solvent revealed that the former fluoresces more strongly at a shorter wavelength, as indicated in Table 1.

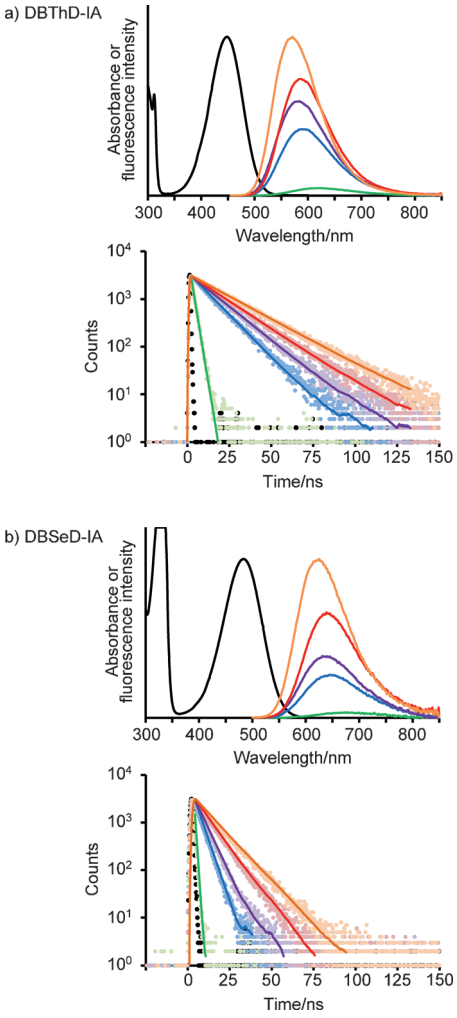

Figure 4. Representative absorption (black, 30 μM) and fluorescence (colored, 5 μM, excited at λ_{abs}) spectra (top) and fluorescence decay curves (5 μM, at λ_{em} with excitation at 456 nm) (bottom) of a) DBThD-IA and b) DBSeD-IA at 25°C in 1,4-dioxane (orange), acetonitrile (black and red), ethanol (purple), methanol (blue), and water (green).

Absorption and fluorescence properties of conventional environment-sensitive fluorophores: The absorption and fluorescence spectra of prodan, ANS-Na, dansylamine, NBD-NHMe, Nile red, and DBD-IA were recorded in binary mixtures of 1,4-dioxane and water (see Figure S1 in the Supporting Information). For comparison, the absorption and fluorescence spectra of DBThD-IA and DBSeD-IA were also recorded in mixtures of 1,4-dioxane and water. The maximum absorption wavelengths, maximum emission wavelengths, and fluorescence quantum yields are presented in Table 2.

Photostabilities of DBThD-IA, DBSeD-IA, and DBD-IA: To evaluate the stabilities of DBThD-IA, DBSeD-IA, and DBD-IA in the excited state, photolysis experiments were

Table 1. Photophysical properties of DBThD-IA and DBSeD-IA in various solvents at 25°C: Maximum absorption wavelength (λ_{abs}), molar absorption coefficient (ε), maximum emission wavelength (λ_{em}), fluorescence quantum yield (Φ_f), fluorescence lifetime (τ_f), fluorescence rate constant (k_f), and non-radiative rate constant (k_{nr}).

Compound	Solvent	D[a]	α[b]	λ_{abs} [nm]	ε [$M^{-1}cm^{-1}$]	λ_{em} [nm]	Φ_f	τ_f [ns]	k_f [10^7 s^{-1}]	k_{nr} [10^7 s^{-1}]
DBThD-IA	*n*-hexane	1.88	0.00	449	8100	537	0.81	22.9	3.5	0.8
	1,4-dioxane	2.24	0.00	448	7700	570	0.73	22.6	3.2	1.2
	ethyl acetate	6.02	0.00	449	7600	573	0.68	21.2	3.2	1.5
	ethanol	24.6	0.83	448	8000	581	0.39	15.2	2.6	4.0
	2,2,2-trifluoroethanol	26.5	1.51	443	9500	590	0.13	7.0	1.8	12
	methanol	32.7	0.93	447	7900	589	0.27	12.0	2.3	6.1
	[D_1]methanol	31.7[c]		447	7800	590	0.39	16.0	2.4	3.8
	acetonitrile	37.5	0.19	448	8000	586	0.49	18.6	2.6	2.7
	DMSO	46.7	0.00	455	8100	598	0.40	14.4	2.8	4.2
	water[d]	80.4	1.17	449	8300	616	0.037	1.90	1.9	51
	deuterium oxide[d]	78.3[e]		449	8200	619	0.10	5.65	1.8	16
DBSeD-IA	*n*-hexane	1.88	0.00	489	7000	591	0.24	11.6	2.1	6.6
	1,4-dioxane	2.24	0.00	485	7000	624	0.14	6.8	2.1	13
	ethyl acetate	6.02	0.00	484	7100	629	0.12	6.3	1.9	14
	ethanol	24.6	0.83	482	7200	638	0.059	3.5	1.7	27
	2,2,2-trifluoroethanol	26.5	1.51	482	8400	645	0.018	1.3	1.4	74
	methanol	32.7	0.93	482	7700	644	0.038	2.5	1.5	38
	[D_1]methanol	31.7[c]		481	7600	648	0.061	3.7	1.7	26
	acetonitrile	37.5	0.19	484	7700	639	0.089	5.3	1.7	17
	DMSO	46.7	0.00	485	7000	653	0.093	4.6	2.0	20
	water	80.4	1.17	486	7700	672	0.0046	0.45	1.0	220
	deuterium oxide	78.3[e]		485	8300	682	0.016	1.1	1.4	89

[a] Dielectric constant of the solvent. [b] Hydrogen-bond donor acidity of the solvent from ref. [62]. DBThD-IA and DBSeD-IA behave only as a hydrogen-bond acceptor because there is no acidic proton in the structure. [c] See ref. [63] . [d] The photophysical data in this solvent is cited from ref. [32]. [e] See ref. [64].

carried out. Figure 5 shows the changes in the absorption spectra of DBThD-IA, DBSeD-IA, and DBD-IA in acetonitrile following photoirradiation with an ultra-high-pressure mercury lamp ($\lambda > 390$ nm).[36] The absorption spectrum of DBThD-IA was largely unchanged following photoirradiation for 20 min, whereas the spectra of DBSeD-IA and DBD-IA showed photodecomposition under the same conditions. To determine whether the photoreactive state was a singlet or a triplet, complementary photolysis experiments were also performed on DBSeD-IA and DBD-IA in deaerated acetonitrile and indicated that the photodecomposition of DBSeD-IA was dramatically suppressed in the absence of dissolved oxygen (see Figure S2 in the Supporting Information). The quantum yields for the photodecomposition were determined in 1,4-dioxane, acetonitrile, methanol, and a mixture of water and methanol (4:1, v/v) by using a previously established method with a spectrofluorimeter and HPLC.[37] As shown in Table 3, the quantum yields were found to be $(1.6–5.9)\times10^{-4}$ for DBThD-IA, $(0.8–12)\times10^{-3}$ for DBSeD-IA, and $(1.7–3.8)\times10^{-3}$ for DBD-IA.[38] These results indicate that DBThD-IA is more stable than DBSeD-IA or DBD-IA under photoirradiation.

Intersystem crossing and internal conversion of DBThD-IA, DBSeD-IA, and DBD-IA: Intersystem crossing and internal conversion were investigated to gain an in-depth understanding of the relaxation process from the first singlet excited (S_1) state of the fluorophores. First, optoacoustic measurements were performed in acetonitrile, methanol, and water as solvent; relatively low signal amplitudes were observed for DBThD-IA, DBSeD-IA, and DBD-IA in all solutions compared with those of the reference solutions (see Figures S3–S5 in the Supporting Information and also the *b* values derived from Equation (5) in the Experimental Section and listed in Table 4). This result indicates that a certain degree of intersystem crossing is involved in the relaxation processes of DBThD-IA, DBSeD-IA, and DBD-IA. The phosphorescence spectra of these fluorophores were then recorded to determine the dissipated energy from the first triplet excited (T_1) state. Although no phosphorescence was observed from DBThD-IA, DBSeD-IA, or DBD-IA, the phosphorescence spectra corresponding to DBThD-IA and DBD-IA could be obtained from DBThD-BTPSA and DBD-BTPSA, which have a sensitizing iridium complex, BTPSA, unit in addition to the fluorescent DBThD-IA or DBD-IA moiety (Figure 6). These iridium complexes were obtained by the condensation of BTPSA with the fluorescent amine with a benzothiadiazole or benzoxadiazole ring (see Scheme S1 in the Supporting Information). Iridium complexes generally show strong phosphorescence, even at room temperature.[39] In DBThD-BTPSA and DBD-BTPSA, triplet–triplet energy transfer occurred from the BTPSA unit to the DBThD-IA and DBD-IA fluorophores. Because the quantum yields for photodecomposition were negligible for DBThD-IA, DBSeD-IA, and DBD-IA (see Table 3), the quantum yields for intersystem crossing (or internal conversion) could be calculated from the *b* values obtained from the optoacoustic measurements, the dissipated energies of the S_1 state (determined from the fluorescence spectra) and the T_1 state (determined from the phosphores-

Table 2. Photophysical properties of DBThD-IA, DBSeD-IA, and conventional environment-sensitive fluorophores in mixtures of 1,4-dioxane and water at 25 °C.

Compound	Water [%, v/v]	λ_{abs} [nm]	λ_{em} [nm]	Φ_f
DBThD-IA	0	448	570	0.73
	25	450	589	0.34
	50	450	600	0.19
	75	450	605	0.089
	100	449	616	0.037
DBSeD-IA	0	485	624	0.14
	25	485	645	0.061
	50	486	654	0.033
	75	487	660	0.015
	100	486	672	0.0046
prodan	0	348	423	0.63
	25	358	489	0.74
	50	372	503	0.58
	75	368	516	0.36
	100	356	529	0.16
ANS-Na	0	376	480	0.48
	25	373	488	0.18
	50	371	501	0.065
	75	367	522	0.015
	100	351	538	0.0021
dansylamine	0	335	487	0.60
	25	334	524	0.48
	50	332	545	0.32
	75	328	556	0.14
	100	325	585	0.062
NBD-NHMe	0	450	520	0.77
	25	466	542	0.38
	50	472	546	0.19
	75	476	558	0.093
	100	478	569	0.042
Nile red	0	522	588	0.94
	25	549	640	0.79
	50	568	653	0.47
	75	585	661	0.23
	100	ND[a]	ND[a]	ND[a]
DBD-IA	0	444	555	0.91
	25	450	584	0.34
	50	452	602	0.17
	75	453	606	0.071
	100	452	616	0.027

[a] Could not be determined because of low solubility.

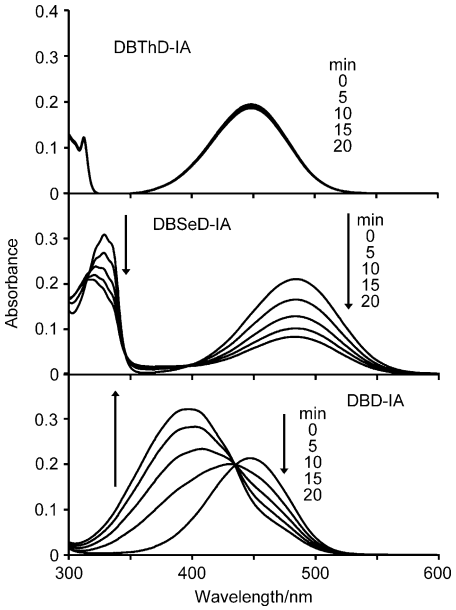

Figure 5. Changes in the absorption spectra of DBThD-IA (24 μM), DBSeD-IA (31 μM), and DBD-IA (20 μM) in acetonitrile upon photoirradiation ($\lambda > 390$ nm) at 25 °C.

Table 3. Photodecomposition quantum yields (Φ_d) for DBD-IA, DBThD-IA, and DBSeD-IA at 25 °C under photoirradiation at 450 nm.

Compound	Solvent	Φ_d
DBThD-IA	1,4-dioxane	0.00024
	acetonitrile	0.00059
	methanol	0.00016
	water/methanol (4:1, v/v)	0.00017
DBSeD-IA	1,4-dioxane	0.0025
	acetonitrile	0.012
	methanol	0.00080
	water/methanol (4:1, v/v)	0.0014
DBD-IA	1,4-dioxane	0.0019
	acetonitrile	0.0038
	methanol	0.0023
	water/methanol (4:1, v/v)	0.0017

cence spectra), and the fluorescence quantum yields (see the Experimental Section).[35] In the photophysical analysis of DBSeD-IA, for which no related phosphorescence spectra could be obtained, we assumed that the energy difference between the S_1 and T_1 states is constant in DBThD-IA and DBSeD-IA (i.e., 2940 cm^{-1}, determined from DBThD-IA and DBThD-BTPSA). Hence, the maximum phosphorescence wavelength of DBSeD-IA is 754 nm. This assumption led to an error in the calculated quantum yield of less than 0.06. The quantum yields for the intersystem crossing and internal conversion and the corresponding rate constants for DBThD-IA, DBSeD-IA, and DBD-IA are presented in Table 4.

Table 4. Nonradiative relaxation of DBThD-IA, DBSeD-IA, and DBD-IA from the excited state at 25 °C; average energy dissipated by fluorescence from the S_1 state ($< E_S >$), the fraction of energy (b), the quantum yields of intersystem crossing (Φ_{isc}) and internal conversion (Φ_{ic}), and the rate constants of intersystem crossing (k_{isc}) and internal conversion (k_{ic}).

Compound	Solvent	$< E_S >$ [cm^{-1}]	b	Φ_{isc}	Φ_{ic}	k_{isc} [10^7 s^{-1}]	k_{ic} [10^7 s^{-1}]
DBThD-IA	acetonitrile	16411	0.671	0.29	0.22	1.6	1.2
	methanol	16311	0.808	0.19	0.54	1.6	4.5
	water	15556	0.846	0.35	0.61	18	32
DBSeD-IA	acetonitrile	15103	0.712	0.72	0.19	14	3.7
	methanol	15002	0.697	0.82	0.14	33	5.6
	water	14498	0.733	0.76	0.24	168	53
DBD-IA	acetonitrile	16612	0.665	0.11	0.23	0.63	1.3
	methanol	16361	0.782	0.24	0.47	2.7	5.3
	water	15556	0.840	0.39	0.59	36	54

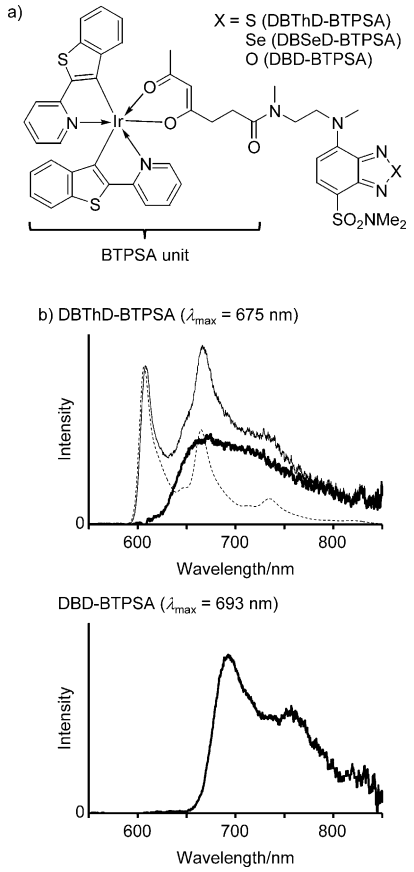

Figure 6. a) Chemical structures of DBD-BTPSA, DBThD-BTPSA, and DBSeD-BTPSA. b) Phosphorescence spectra of DBThD-BTPSA and DBD-BTPSA in 2-methyltetrahydrofuran at 77 K. Because the phosphorescence from DBThD-BTPSA originates from both the DBThD and BTPSA units, the phosphorescence spectrum of BTPSA (dotted line) was subtracted from that of DBThD-BTPSA (thin solid line) to obtain the spectrum of the DBThD moiety (thick solid line). The absorption of each sample was adjusted to approximately 0.2 at 450 nm.

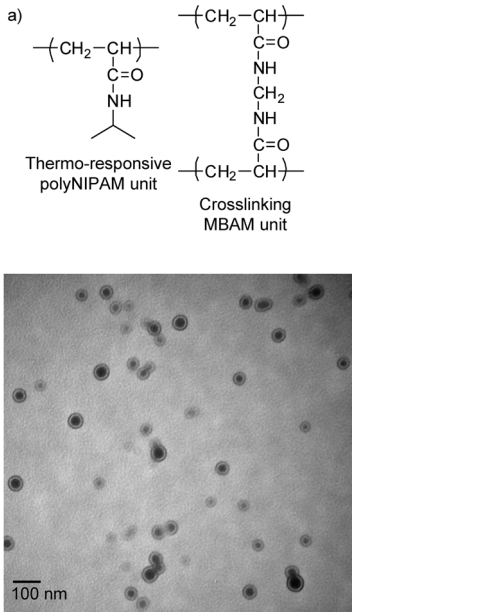

Figure 7. a) Chemical structures of a thermoresponsive polyNIPAM unit and a crosslinking MBAM unit. b) TEM image of the DBThD nanogels in the dried state. The diameter of the DBThD nanogels was 48.4 ± 6.4 nm (mean ± s.d.).

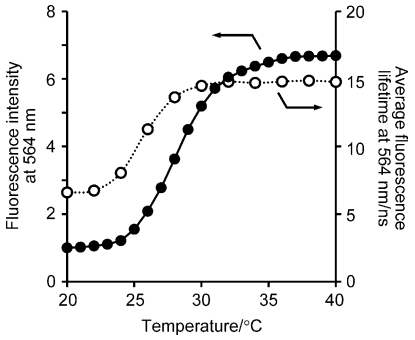

Figure 8. Behavior of the DBThD nanogel (0.002 w/v %) in the COS7 cell extract. Variation in the fluorescence intensity (●) and lifetime (○) with temperature.

Application of DBThD-IA in a fluorescent nanogel thermometer for intracellular thermometry: The high environmental sensitivity and enhanced photostability of DBThD-IA allowed us to develop a new fluorescent nanogel thermometer for intracellular thermometry by using this new fluorophore. In a previous study we developed a fluorescent nanogel thermometer consisting of a thermoresponsive polyNIPAM unit and a crosslinking MBAM unit (Figure 7) in addition to a fluorescent DBD-IA unit.[34] In this study the DBD-IA unit in the fluorescent nanogel thermometer was replaced by the DBThD-IA unit to improve the photostability of the thermometer during intracellular thermometry. The corresponding fluorescent monomer, DBThD-AA, was synthesized and a fluorescent nanogel thermometer containing DBThD-IA units (termed "DBThD nanogel" in this paper) was prepared. The size of the DBThD nanogel was measured by TEM (Figure 7) and dynamic light scattering (see Figure S6 in the Supporting Information). The fluorescence response of the DBThD nanogel to temperature variations was examined in a COS7 cell extract (Figure 8) and KCl aqueous solutions (0–200 mM, see Figure S7 in the Supporting Information). As shown in Figure 8, the fluorescence intensity of the DBThD nanogel increased 5.9-fold in the COS7 cell extract when the solution temperature was increased from 23 to 35 °C. Conversely, the fluorescence lifetime of the DBThD nanogel extended from 6.6 to 14.8 ns as the temperature increased from 20 to 32 °C.[40] Finally, the functionality of the DBThD nanogel inside living COS7 cells was assessed after microinjection of the nanogel into the cytoplasm. The DBThD nanogels exhibited remarkable photostability (Figure 9), retaining their sensitivity to changes in cellular temperature (see Figure S8 in the Supporting Information). At 36 °C, the photodecomposition rate of the DBThD nanogels was only 22 % of that of the originally reported DBD nanogels. Note that the photodecompo-

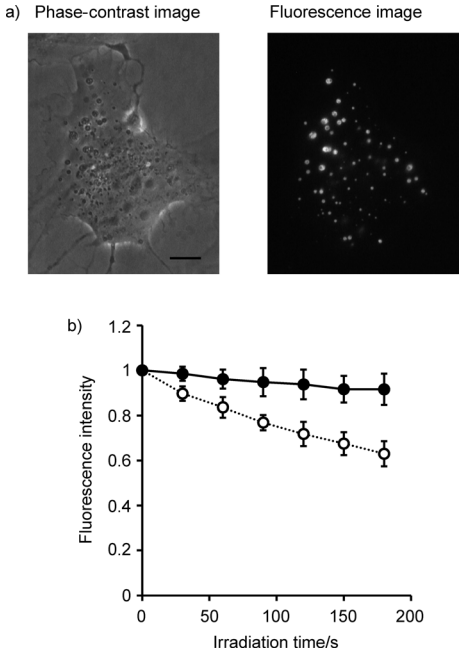

Figure 9. a) Phase-contrast and fluorescence images of a living COS7 cell containing the DBThD nanogels. Bar: 10 μm. b) Photostability of the DBThD (●) and the DBD nanogels (○) in living COS7 cells at 36 °C upon continuous photoirradiation at 488 nm (laser power at the sample plane: 63.5 μW). The total fluorescence intensity of the nanogels inside a cell at 0 s was set to unity and averaged for 7 cells (for DBThD nanogels) or 10 cells (for DBD nanogels). Error bar: ± s.d.

sition of the DBThD nanogels was accelerated at higher temperatures. The magnitude of the photodecomposition of the DBThD nanogels inside COS7 cells at 23 °C was 63 % of that at 36 °C. In conclusion, the new environment-sensitive fluorophore DBThD-IA successfully improves the photostability of the fluorescent nanogel thermometer.

Discussion

Solvent effects on the fluorescence properties of DBThD-IA and DBSeD-IA: As summarized in Table 1, the maximum emission wavelengths of DBThD-IA and DBSeD-IA shift bathochromically in polar solvents, whereas the absorption wavelengths of these compounds are relatively unchanged regardless of the solvent. This feature can be ascribed to the intramolecular charge transfer (ICT) character of the excited state of DBThD-IA and DBSeD-IA, which contain both electron-pushing and -pulling systems within a single molecule.[41] As a result of the excitation, the dipole moments of DBThD-IA and DBSeD-IA increase with electron transfer from the amino substituent to the benzothiadiazole or benzoselenadiazole ring.[42] Because a greater stabilization of the energy level is provided between a solute with a larger dipole moment and a more polar solvent, the maximum emission wavelengths of DBThD-IA and DBSeD-IA are redshifted when the polarity of the solvent is increased.

The fluorescence quantum yields of DBThD-IA and DBSeD-IA are affected by the polarity and hydrogen-bonding ability of the solvents. The calculated fluorescence and nonradiative rate constants (k_f and k_{nr} in Table 1) indicate that the variation in the fluorescence quantum yield of these fluorophores as a function of solvent is due to a difference in the nonradiative rate constant but not the fluorescence rate constant. Figure 10 shows the relationship between the k_{nr} value of the nonradiative relaxation process and the maximum emission energy. In aprotic solvents (●), a good linear relationship (known as the "energy-gap law"[43]) is observed for both DBThD-IA and DBSeD-IA. Thus, it can be concluded that the polarity of the solvent influences the fluorescence quantum yield of DBThD-IA and DBSeD-IA. In protic solvents (○), the calculated k_{nr} values are larger than those expected based on the energy-gap law. This discrepancy indicates that the hydrogen bonding between the fluorophore and the solvent molecule(s) contributes to the nonradiative relaxation process. The effects of the hydrogen bonding on the nonradiative relaxation process were also confirmed by deuterium isotope effects.[44] For instance, the k_{nr} value of DBThD-IA in [D_1]methanol ($3.8\times10^7\ s^{-1}$) is 63 % of that in methanol, and that in deuterium oxide ($1.6\times10^8\ s^{-1}$) is 31 % of that in water, which indicates that hydrogen bonding with solvent molecules promotes the nonradiative relaxation of DBThD-IA. Similar deuterium isotope effects were also observed for the k_{nr} value of DBSeD-IA. Based on our previous research regarding solvent effects on the photophysical properties of DBD-IA,[32] the hydrogen-bonding sites in DBThD-IA and DBSeD-IA are thought to be the nitrogen atoms in the benzothiadiazole and benzoselenadiazole rings, respectively, in addition to the oxygen atoms in the dimethylsulfamoyl group of the substituent. In

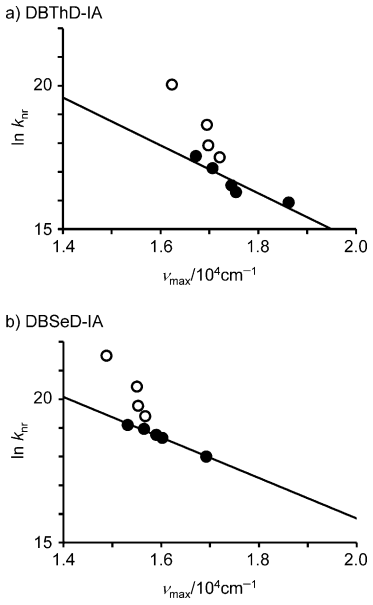

Figure 10. Relationship between the nonradiative rate constant and the maximum emission number for a) DBThD-IA and b) DBSeD-IA in aprotic (●) and protic (○) solvents.

summary, the fluorescence properties of DBThD-IA and DBSeD-IA are influenced by the polarity of the environment and hydrogen bonding with solvent molecules, and they fluoresce strongly in both apolar and aprotic solvents.

Comparison of the fluorescence properties of DBSeD-IA and DBThD-IA (or of DBSeD-IA and DBD-IA): The absorption and emission wavelengths of DBSeD-IA are longer than those of DBThD-IA and DBD-IA by 30–57 nm. Thus, the selenium atom in benzoselenadiazole has different effects on the absorption and fluorescence properties than the sulfur atom in benzothiadiazole and the oxygen atom in benzoxadiazole. The reason for this difference is thought to be the involvement of a d-orbital electron in the excitation and fluorescence processes. Similar effects of the selenium atom have been reported for the absorption wavelengths of nonsubstituted benzoxadiazole analogues[45] and the absorption and emission wavelengths of rhodamine[46] and alkylthiobenzoxadiazole analogues,[47] although a sulfur atom also produces a bathochromic shift in comparison with an oxygen atom in the case of the rhodamine analogues. In addition, the fluorescence quantum yield of DBSeD-IA is smaller than that of DBThD-IA (by one eighth to one third, depending on the solvent), whereas this difference was not observed between DBThD-IA and DBD-IA (see Table 1 and ref. [32]). The effects of the selenium atom on the fluorescence quantum yield could be ascribed to the heavy atom effect,[45,48] which promotes intersystem crossing as a nonradiative relaxation process competing with the fluorescence (cf. the spin–orbit coupling constants of oxygen, sulfur, and selenium are 154, 365, and 1659 cm^{-1}, respectively[49]). In fact, our optoacoustic measurements revealed that the quantum yield for intersystem crossing in DBSeD-IA (e.g., 0.82 in methanol) is higher than those of DBThD-IA (0.19) and DBD-IA (0.24).

Comparison of the environmental sensitivity of the new and conventional environment-sensitive fluorophores: In this study, the sensitivity of a fluorophore to the surrounding environment was evaluated by using the ratio of the fluorescence quantum yields in 1,4-dioxane and water (for original data, see Table 2). In principle, this ratio of fluorescence quantum yields reflects the sensitivity of stimulus-responsive fluorescent sensors containing the environment-sensitive fluorophores. The ratios of the fluorescence quantum yields decrease in the order ANS-Na (230) > DBD-IA (33.9) > DBSeD-IA (31.1) > DBThD-IA (19.7) > NBD-NHMe (18.3) > dansylamine (9.6) > prodan (4.0). Thus, the new fluorophores, DBThD-IA and DBSeD-IA, have moderate sensitivity to their environment. When an environment-sensitive fluorophore is incorporated into a stimulus-responsive macromolecule to develop a fluorescent sensor for an intracellular monitoring system, the most sensitive ionized ANS-Na can easily suffer from undesirable interactions with cellular molecules because of its static electric charge. In addition, the excitation of ANS-Na, dansylamine, and prodan at short wavelengths (less than 400 nm) can cause serious damage to a living cell. Therefore we concluded that DBThD-IA and DBSeD-IA are good candidates as environment-sensitive fluorophores for a component of an intracellular fluorescent sensing system based on a stimulus-responsive macromolecule.

Comparison of the photostabilities of DBThD-IA, DBSeD-IA, and DBD-IA: The most important finding in this research has been that DBThD-IA is more stable than DBD-IA under photoirradiation. The reason for this difference is unclear, but it is assumed to be a result of the variation in the bond dissociation energy of the N–S bond in the benzothiadiazole ring and the N–O bond in the benzoxadiazole ring, based on the literature regarding the photodecomposition processes of nonsubstituted benzoxadiazole[50] and 4,7-dimethyl-2,1,3-benzoxadiazole.[51] The high photostability of DBThD-IA encouraged us to create a DBThD nanogel as a photostable fluorescent thermometer for intracellular thermometry. In contrast to DBThD-IA, the photostability of DBSeD-IA is comparable to that of DBD-IA (see Table 3). Complementary photolysis experiments (see Figure S2 in the Supporting Information) indicated that the photodecomposition of DBSeD-IA is initiated by a reaction with oxygen in the triplet excited state and does not involve the singlet excited state. Conversely, dissolved oxygen was not observed to influence the photolysis experiment of DBD-IA, which suggests that the photodecomposition of DBD-IA occurs from the singlet excited state. This conclusion is supported by the photodecomposition mechanism of 1,2,5-oxadiazoles reported in the literature.[52] Although they have similar structures, DBSeD-IA and DBD-IA undergo photolysis by different mechanisms.

Functional improvement of a fluorescent nanogel thermometer by using DBThD-IA as an environment-sensitive fluorophore: Recent progress in fluorescent molecular thermometers has inevitably triggered an explosion of temperature measurements in extremely small spaces.[53] In particular, a fluorescent polymeric thermometer that combines a thermoresponsive polymer and an environment-sensitive fluorophore offers unprecedented sensitivity to variations in temperature and thus can be used to detect subtle changes in intracellular temperature.[34] Functional improvements in the fluorescent polymeric thermometer, gelation,[34,54] modification of functional temperature ranges,[33b,d,55] and the promotion of solubility[33d,34] have been achieved by optimizing the chemical structure of a thermoresponsive polymer. Similarly, changing the environment-sensitive fluorophore in the fluorescent polymeric thermometer resulted in an increase in sensitivity and a bathochromic shift of the excitation wavelength.[56] This report describes the first study to improve the photostability of a fluorescent polymeric thermometer. As shown in Figure 9, the DBThD nanogel has a 4.8-fold greater durability in living COS7 cells than our original fluorescent nanogel thermometer, the DBD nanogel. When an intracellular thermometry is conducted, this improved photostability of the fluorescent polymeric ther-

mometer will be quite helpful because more reliable and long-term temperature monitoring can be achieved. Finally, we expect that the new environment-sensitive fluorophore developed in this study, DBThD-IA, can make fluorescent polymeric thermometers more accessible to biologists who are trying to correlate intracellular temperatures with various cellular events.

In this study, we synthesized the new fluorophores DBThD-IA and DBSeD-IA and used their absorption, fluorescence, and phosphorescence spectra, and their optoacoustic signals to examine their photophysical and photochemical properties. Both DBThD-IA and DBSeD-IA showed environment-sensitive fluorescence that was efficient in apolar and aprotic solvents, and DBThD-IA also indicated good photostability. These characteristics allowed us to use DBThD-IA as an environment-sensitive fluorophore to develop a new fluorescent nanogel thermometer. To perform accurate thermometry measurements of cells and tissues in the future, we are investigating useful fluorescent thermometers containing DBThD-IA with the aim of creating another environment-sensitive fluorophore that can be excited around a red or near-infrared region.

Experimental Section

Materials and apparatus: DBD-IA (*N*,2-dimethyl-*N*-(2-{methyl[7-(dimethylsulfamoyl)-2,1,3-benzoxadiazol-4-yl]amino}ethyl)propanamide),[32] DBThD-IA (*N*,2-dimethyl-*N*-(2-{methyl[7-(dimethylsulfamoyl)-2,1,3-benzothiadiazol-4-yl]amino}ethyl)propanamide),[32] NBD-NHMe (4-methylamino-7-nitro-2,1,3-benzoxadiazole),[4b] and the DBD nanogel[34] were obtained as previously reported. ANS-Na (sodium 8-anilino-1-naphthalenesulfonate), dansylamine (1-(dimethylamino)-5-naphthalenesulfonamide), isobutyric anhydride, and Nile red (9-diethylamino-5*H*-benzo[*a*]phenoxazine-5-one) were purchased from TCI. Prodan (6-propionyl-2-(dimethylamino)naphthalene) was purchased from AnaSpec. Acetonitrile, 1,4-dioxane, DMSO, ethyl acetate, *n*-hexane, and methanol were of spectrophotometric grade (Dojindo or Wako Pure Chemicals). Ethanol (dehydrated, 99.5%), rhodamine B, and NIPAM (*N*-isopropylacrylamide) were purchased from Wako Pure Chemicals. 2,2,2-Trifluoroethanol was obtained from Acros. [D_1]Methanol (CH_3OD; 99.5 atom% D), deuterium oxide (99.9 atom% D), and MBAM (*N*,*N*′-methylenebis(acrylamide)) were purchased from Sigma–Aldrich. Water was purified by using a Milli-Q reagent system, Direct-Q 3 UV (Millipore). The solvents were aerated unless otherwise noted. All other reagents were of reagent grade and used without further purification.

^{1}H NMR spectra were obtained by using a Bruker Avance 400 spectrometer. *J* values are given in hertz. Mass spectra acquired with an electrospray ionization (ESI) system were recorded with a Bruker micrOTOF-05 spectrometer. The melting points were measured with a Yanagimoto Micro Melting Point Apparatus or a Round Science RFS-10 and are uncorrected.

Synthesis: The synthesis procedures for the iridium complex, BTPSA (bis(2-(2′-benzothienyl)pyridinato-N,$C^{3'}$)iridium(succinylacetonate)), and its derivatives (DBThD-BTPSA, DBSeD-BTPSA, and DBD-BTPSA) are described in the Supporting Information.

4-Chloro-2,1,3-benzoselenadiazole: 1-Chloro-2,3-diaminobenzene (600 mg, 4.21 mmol)[57] was dissolved in ethanol (6 mL). After the addition of selenium dioxide (490 mg, 4.42 mmol) in hot ethanol (10 mL), the mixture was stirred at 80 °C for 30 min. The reaction mixture was then evaporated under reduced pressure and the residue was purified by column chromatography on silica gel with dichloromethane/*n*-hexane (1:1) as eluent to produce 4-chloro-2,1,3-benzoselenadiazole (905 mg, 99%) as a white powder. M.p. 163–164 °C (lit.:[58] 158–161 °C); ^{1}H NMR (400 MHz, $CDCl_3$): $\delta = 7.78$ (dd, $J(H,H) = 9.0$, 1.0 Hz, 1H), 7.53 (dd, $J(H,H) = 7.0$, 1.0 Hz, 1H) 7.43 ppm (dd, $J(H,H) = 7.0$, 9.0 Hz, 1H); ^{13}C NMR (100 MHz, $CDCl_3$): $\delta = 160.5$, 157.4, 129.4, 128.2, 127.9, 122.4 ppm; HRMS (ESI): *m*/*z* calcd for $C_6H_4ClN_2Se + H^+$: 218.9228 $[M+H]^+$; found: 218.9232; elemental analysis calcd (%) for $C_6H_3ClN_2Se$: C 33.13, H 1.39, N 12.88; found: C 33.46, H 1.62, N, 12.76.

7-Chloro-2,1,3-benzoselenadiazole-4-sulfonyl chloride: 4-Chloro-2,1,3-benzoselenadiazole (600 mg, 2.76 mmol) was dissolved in chlorosulfuric acid (5 mL) at 0 °C. The mixture was stirred at 0 °C for 1 h and then heated at 150 °C for 3 h. After the reaction, the mixture was poured into ice/water (300 mL) and the product was extracted with dichloromethane (200 mL × 2). The organic layer was dried over Na_2SO_4 and was evaporated to dryness under reduced pressure. The residue was purified by column chromatography on silica gel with dichloromethane as eluent to produce 7-chloro-2,1,3-benzoselenadiazole-4-sulfonyl chloride (574 mg, 66%) as a white powder. M.p. 220 °C (decomp.); ^{1}H NMR (400 MHz, $CDCl_3$): $\delta = 8.31$ (d, $J(H,H) = 7.6$ Hz, 1H), 7.74 ppm (d, $J(H,H) = 7.6$ Hz, 1H); ^{13}C NMR (100 MHz, $CDCl_3$): $\delta = 157.6$, 152.5, 136.8, 134.7, 132.4, 126.0 ppm; HRMS (ESI): *m*/*z* calcd for $C_6H_3Cl_2N_2O_2SSe + H^+$: 316.8457 $[M+H]^+$; found: 316.8456; elemental analysis calcd (%) for $C_6H_2Cl_2N_2O_2SSe$: C 22.80, H 0.64, N 8.86; found: C 22.98, H 0.89, N 8.88.

7-Chloro-*N*,*N*-dimethyl-2,1,3-benzoselenadiazole-4-sulfonamide (DBSeD-Cl): 7-Chloro-2,1,3-benzoselenadiazole-4-sulfonyl chloride (300 mg, 0.949 mmol) was dissolved in dichloromethane (20 mL). After the addition of a mixture of 50% dimethylamine solution (0.5 mL) and acetonitrile (1.5 mL), the resultant solution was stirred at room temperature for 30 min. After the reaction, the mixture was evaporated to dryness under reduced pressure and the residue was purified by column chromatography on silica gel with dichloromethane as eluent to produce DBSeD-Cl (261 mg, 85%) as a white powder. M.p. 201–202 °C; ^{1}H NMR (400 MHz, $CDCl_3$): $\delta = 8.15$ (d, $J(H,H) = 7.4$ Hz, 1H), 7.65 (d, $J(H,H) = 7.6$ Hz, 1H), 2.96 ppm (s, 6H); ^{13}C NMR (100 MHz, $CDCl_3$): $\delta = 157.7$, 154.9, 133.1, 130.9, 126.9, 126.8, 37.9 ppm; HRMS (ESI): *m*/*z* calcd for $C_8H_9ClN_3O_2SSe + H^+$: 325.9269 $[M+H]^+$; found: 325.9260, elemental analysis calcd (%) for $C_8H_8ClN_3O_2SSe$: C 29.60, H 2.48, N 12.94; found: C 29.75, H 2.53, N 12.98.

***N*,*N*-Dimethyl-7-{methyl[2-(methylamino)ethyl]amino}-2,1,3-benzoselenadiazole-4-sulfonamide**: DBSeD-Cl (70 mg, 0.216 mmol) was dissolved in acetonitrile (4 mL). After the addition of *N*,*N*′-dimethylethylenediamine (1 mL), the mixture was heated at 80 °C for 1 h. The reaction mixture was then evaporated under reduced pressure and the residue was purified by column chromatography on silica gel with dichloromethane/methanol (5:1) as eluent to produce *N*,*N*-dimethyl-7-{methyl[2-(methylamino)ethyl]amino}-2,1,3-benzoselenadiazole-4-sulfonamide (81 mg, >99%) as a red oil. ^{1}H NMR (400 MHz, [D_6]DMSO): $\delta = 7.80$ (d, $J(H,H) = 8.4$ Hz, 1H), 6.30 (d, $J(H,H) = 8.4$ Hz, 1H), 4.03 (t, $J(H,H) = 6.8$ Hz, 2H), 3.36 (s, 3H), 2.78 (t, $J(H,H) = 6.8$ Hz, 2H), 2.69 (s, 6H), 2.29 ppm (s, 3H); ^{13}C NMR (100 MHz, [D_6]DMSO): $\delta = 147.1$, 144.5, 142.5, 139.3, 104.8, 101.6, 53.8, 49.2, 40.9, 37.4, 36.1 ppm; HRMS (ESI): *m*/*z* calcd for $C_{12}H_{20}N_5O_2SSe + H^+$: 378.0503 $[M+H]^+$; found: 378.0514.

***N*,2-Dimethyl-*N*-(2-{methyl[7-(dimethylsulfamoyl)-2,1,3-benzoselenadiazol-4-yl]amino}ethyl)propanamide (DBSeD-IA)**: *N*,*N*-Dimethyl-7-{methyl-[2-(methylamino)ethyl]amino}-2,1,3-benzoselenadiazole-4-sulfonamide (71.8 mg, 191 μmol) was dissolved in dichloromethane (25 mL). After the addition of triethylamine (TEA; 26.6 μL, 191 μmol) and isobutyric anhydride (47.7 μL, 286 μmol), the mixture was stirred at room temperature for 17 min. Na_2CO_3 (1 g) was then added to the reaction mixture and after filtration the resultant mixture was poured into dichloromethane (100 mL). The organic layer was washed with a 0.1 M NaOH aqueous solution (50 mL × 2) and water (50 mL × 2). The organic layer was dried over Na_2SO_4 and evaporated to dryness under reduced pressure. The residue was purified by column chromatography on silica gel with dichloromethane/methanol (100:1) as eluent to produce DBSeD-IA (58 mg, 68%) as a red powder. M.p. 126–127 °C; ^{1}H NMR (400 MHz, $CDCl_3$): $\delta = 8.09$, 8.05 (d, $J(H,H) = 8.4$ Hz, 1H), 6.30, 6.28 (d, $J(H,H) = 8.4$ Hz, 1H), 4.36, 4.24 (t, $J(H,H) = 6.8$ Hz, 2H), 3.79, 3.73 (t, $J(H,H) = 6.8$ Hz, 2H), 3.29, 3.20 (s, 3H), 3.04, 3.02 (s, 3H), 2.91, 2.88 (s,

6H), 2.67 (q, 1H) 1.11, 0.99 ppm (d, J(H,H) = 6.8 Hz, 6H); ^{13}C NMR (100 MHz, $CDCl_3$): δ = 177.4, 177.2, 157.2, 154.0, 147.1, 146.8, 137.4, 137.0, 118.4, 117.1, 103.5, 103.2, 53.2, 51.6, 48.8, 46.9, 41.3, 41.1, 36.1, 34.3, 30.3, 30.0, 19.8, 19.0 ppm; HRMS (ESI): m/z calcd for $C_{16}H_{26}N_5O_3SSe+H^+$: 448.0922 $[M+H]^+$; found: 448.0926.

***N*-(2-{[7-(*N*,*N*-Dimethylaminosulfonyl)-2,1,3-benzothiadiazol-4-yl]-(methyl)amino}ethyl)-*N*-methylacrylamide (DBThD-AA)**: *N*,*N*-Dimethyl-7-{methyl[2-(methylamino)ethyl]amino}-2,1,3-benzothiadiazole-4-sulfonamide (118.6 mg, 0.36 mmol)[32] was dissolved in acetonitrile (8 mL). After the addition of triethylamine (50.3 μL, 0.36 mmol) and acryloyl chloride (38.0 μL, 0.47 mmol) at 0 °C, the mixture was stirred at 0 °C for 60 min. Na_2CO_3 (1 g) was then added to the reaction mixture and after filtration the organic layer was dried over Na_2SO_4 and evaporated to dryness under reduced pressure. The residue was purified by column chromatography on silica gel with dichloromethane/methanol (200:1→10:1) as eluent to produce DBThD-AA (113.6 mg, 82%) as an orange powder. M.p. 144–145 °C; ^{1}H NMR (400 MHz, $CDCl_3$): δ = 8.10 (d, J(H,H) = 8.4 Hz, 1H), 6.27–6.59 (m, 3H), 5.68, 5.62 (d, J(H,H) = 10.4 Hz, 1H), 4.36, 4.27 (t, J(H,H) = 6.8 Hz, 2H), 3.86, 3.81 (t, J(H,H) = 6.8 Hz, 2H), 3.34, 3.22 (s, 3H), 3.11 (s, 3H), 2.90, 2.88 ppm (s, 6H); ^{13}C NMR (100 MHz, $CDCl_3$): δ = 166.6, 152.5, 147.3, 145.7, 145.2, 136.1, 135.9, 128.3, 128.2, 127.2, 127.0, 115.9, 114.9, 104.1, 104.0, 52.8, 51.4, 49.1, 46.9, 41.2, 40.7, 37.9, 36.5, 34.5 ppm; HRMS (ESI): m/z calcd for $C_{15}H_{22}N_5O_3SSe+H^+$: 432.0609 $[M+H]^+$; found: 432.0598.

Photophysical studies of the environment-sensitive fluorophores: UV/Vis absorption spectra (5–30 μM) were recorded at 25 °C with a JASCO V-550 UV/Vis spectrophotometer. Fluorescence spectra (0.1–30 μM) were recorded with a JASCO FP-6500 spectrofluorimeter with a Hamamatsu R-7029 optional photomultiplier tube (operative range, 200–850 nm) and were corrected by using a JASCO ESC-333 substandard light source at 25 °C. The fluorescence quantum yields (Φ_f) were determined from Equation (1) in which F is the area under the corrected fluorescence spectrum obtained with excitation at a specific wavelength, A is the absorbance at that wavelength, n is the refractive index of the solvent, and the subscripts R and S represent the reference and the sample, respectively. Quinine sulfate (Φ_f = 0.577 in 0.1 N H_2SO_4)[59] and rhodamine 6G (Φ_f = 0.94 in ethanol)[60] were used as references.

$$\Phi_{f,S} = \Phi_{f,R} F_S A_R n_S^2 / F_R A_S n_R^2 \quad (1)$$

The fluorescence lifetimes (τ_f) were determined by using a time-correlated single-photon counting (TCSPC) fluorimeter, FluoroCube 300U (Horiba Jobin Yvon), at 25 °C. The samples were excited with an LED (NanoLED-456, Horiba, 456 nm) at a repetition rate of 1 MHz. The recorded fluorescence decay curves ($I(t)$) were well fitted by a single-exponential function expressed as Equation (2), in which B is the pre-exponential factor and t is the time.

$$I(t) = B\exp(-t/\tau_f) \quad (2)$$

The steady-state photolysis study was performed by using an ultra-high-pressure mercury lamp (USHIO, 250 W) as the light source with a cutoff filter. The absorbance of each sample solution was adjusted to approximately 0.20 at the maximum absorption wavelength. The photoirradiation was performed on a vigorously stirred sample solution in a quartz cell. The primary photodecomposition quantum yields of DBThD-IA, DBSeD-IA, and DBD-IA were determined in 1,4-dioxane, acetonitrile, methanol, and a mixture of water and methanol (4:1, v/v) by using a JASCO FP-6500 spectrofluorimeter and HPLC. This method was established in our previous research[37] and the details, with modifications, are described below. The HPLC system consisted of a JASCO PU-2080 pump, a Hitachi L-4000H UV detector, and a JASCO CO-2060 column thermostat. DBThD-IA, DBSeD-IA, or DBD-IA was dissolved in the solvent and its absorbance was adjusted to 0.3 at 450 nm. The sample solution (3.2 mL) was stirred at 25 °C during photoirradiation with monochromatic light at 450 nm in the spectrofluorimeter (bandpass: 10 nm). At specific intervals, an aliquot (10 μL) of the solution was subjected to HPLC. The photoreaction mixture was separated by using an analytical column, Wako Wakosil II5C18AR (4.6 × 150 mm, i.d., 5 μm), and an isocratic eluent (a mixture of water and acetonitrile) at a flow rate of 1.0 mL min^{-1}. The eluted liquid was monitored by UV spectrophotometry (450 nm for DBThD-IA and DBD-IA, 470 nm for DBSeD-IA). The ratio S'/S, in which S is the peak area of the fluorescent compound in the aliquot before photoirradiation and S' is the peak area of the fluorescent compound in the aliquot after photoirradiation, varied linearly with the photoirradiation time t (min) according to Equation (3) in which ε_{450nm} is the molecular extinction coefficient at 450 nm and a is the relative photodecomposition efficiency.

$$S'/S = 1 - a\varepsilon_{450nm} t \quad (3)$$

The relative photodecomposition efficiency a was calculated from the values of t and S'/S by least-squares analyses. All least-square analyses were performed by using Microsoft Excel. The primary photodecomposition quantum yields were obtained by comparing the a values with the photodecomposition efficiency of a reference compound, 5-dimethylamino-2,1,3-benzoxadiazole, at 275 nm (photodecomposition quantum yield, 0.21 in acetonitrile).[37] Rhodamine B was used as an actinometer.[61]

Time-resolved optoacoustic measurements were performed to determine the quantum yields of intersystem crossing (Φ_{isc}). The fourth harmonic (266 nm) of a Nd^{3+}:YAG laser (Spectra-Physics GCR-130, pulse width 6 ns) was used as the excitation source. Optoacoustic signals originating from the radiationless transitions of solute molecules were detected by using a piezoelectric transducer (Panametrics Model V103, 1 MHz) and fed into a high-gain (40 dB) preamplifier (Panametrics Model 5676). The output voltage was then input into a digitizing oscilloscope (Tektronix TDS-540, 500 MHz, 2 G samples/s) connected to a personal computer (Dell GXM 5200). The fluence of the laser pulses was varied by a neutral density filter and measured with a pyroelectric energy meter (Laser Precision RjP 735 and Rj 7610). The absorbance of each sample solution was adjusted to 0.1 at 266 nm. The intensity (H) of the optoacoustic signal results from two variations in the tested solution during a heat integration time, namely, a thermally induced volume change (ΔV_{th}) and a structural volume change (ΔV_r).[35] Thus, H can be expressed by Equation (4) in which k is an instrumental constant that depends on the geometric arrangement and solution constants such as density and sound velocity.

$$H = k(\Delta V_{th} + \Delta V_r) \quad (4)$$

In this analysis, the contribution of the structural volume change (ΔV_r) can be ignored because neither bond dissociation nor bond formation were induced by the photoexcitation and also because the change in the solvation due to triplet formation was negligible. Therefore, H is related only to ΔV_{th} (contraction/expansion of the solvent due to the heat released in the relaxation process of the solute) and can be expressed by Equation (5) in which K is a constant related to the thermoelastic properties of the solution and instrumental factors, E_L is the laser pulse fluence, A is the absorbance of the sample solution, and b is the fraction of energy deposited in the medium as prompt heat within the time resolution of the experiment.

$$H = KE_L b(1-10^{-A}) \quad (5)$$

Because the values of b for the reference compounds 2-hydroxybenzophenone (in acetonitrile and methanol) and sodium dichromate (in water) can be assumed to be unity, the value of b of the sample compound can be determined by comparing the slope of the linear relationship between the signal amplitude and the laser power. To determine the value of Φ_{isc}, Equation (6) based on the energy balance[34] can be used in which E_λ is the photon energy and $<E_S>$ and E_T are the average energy dissipated by fluorescence from the S_1 state and the energy of the lowest excited triplet state, respectively.

$$E_\lambda b = E_\lambda - \Phi_f <E_S> - \Phi_{isc} E_T \quad (6)$$

The E_T value was determined from the phosphorescence spectra recorded with excitation at 450 nm in 2-methyltetrahydrofuran at 77 K. Because

the contribution of the photochemical reaction from the S_1 state was negligible, the quantum yield of internal conversion (Φ_{ic}) was calculated from the relation $\Phi_f+\Phi_{isc}+\Phi_{ic}=1$.

Preparation and characterization of the DBThD nanogel: NIPAM (2 mmol), MBAM (20 μmol), DBThD-AA (20 μmol), and *N*,*N*,*N*′,*N*′-tetramethylethylenediamine (TMEDA, 58 μmol) were dissolved in a solution of sodium dodecyl sulfate (12.6 mM, 20 mL). Dry argon gas was injected into the solution for 30 min to remove dissolved oxygen. Ammonium persulfate (APS, 560 μmol) was added to initiate the emulsion polymerization and the mixture was stirred at 70 °C with a rod with a paddle at 250 rpm for 4 h under an argon atmosphere. The mixture was then poured into water (400 mL) and nanogels were precipitated by using a salting-out technique. After purification by dialysis, the nanogel dispersion was freeze-dried to afford the DBThD nanogel (223 mg, 94 %) as a pale-yellow powder.

The amount of fluorescent DBThD-IA units in the DBThD nanogels was evaluated on the basis of their corresponding concentrations when dissolved at 0.01 w/v % in water, and it was determined to be 4.0 μM from the absorbances of a methanolic solution of the nanogels by comparison with DBThD-IA as a model compound.

A TEM image was obtained with a Hitachi H-7100 transmission electron microscope. A drop of the DBThD nanogel solution in ethanol (0.01 w/v %, 5 μL) was allowed to settle on a Formvar-coated copper grid. The specimen was air-dried at room temperature and then examined at an accelerating voltage of 75 kV. The hydrodynamic diameter was estimated from dynamic light scattering (DLS) measurements with a Zetasizer Nano ZS apparatus (Malvern Instruments). The samples (0.001 w/v %) were equilibrated at each temperature for 5 min.

The fluorescence intensities and lifetimes of the DBThD nanogels at specific temperatures were measured with JASCO FP-6500 and Horiba FluoroCube 300U instruments, respectively, as described above. The temperature of the samples was controlled with a JASCO ETC-273T temperature controller. In the fluorescence lifetime measurements, the fluorescence decay curves were best fitted by a double-exponential function given by Equation (7).

$$I(t) = B_1\exp(-t/\tau_1) + B_2\exp(-t/\tau_2) \quad (7)$$

The average fluorescence lifetime ($<\tau_f>$) was calculated from Equation (8).

$$<\tau_f> = (B_1{\tau_1}^2 + B_2{\tau_2}^2)/(B_1\tau_1 + B_2\tau_2) \quad (8)$$

Fluorescence imaging: COS7 cells (African Green Monkey SV40-transformed kidney fibroblast cell line) were cultured on a 35 mm glass-based dish (ASAHI Techno GLASS) in Dulbecco's modified Eagle medium (DMEM, Gibco No. 11965) supplemented with 5 % fetal bovine serum (Gibco), penicillin/streptomycin (Gibco), L-glutamine (Gibco), sodium pyruvate (Gibco), and nonessential amino acids (Gibco). Before live cell imaging, the medium was replaced with phenol red-free culture medium (2 mL, Gibco No. 21063 was used instead of No. 11965 in the above procedure). The temperature of the culture medium was controlled by using a stage plate heater (TOKAI HIT) and a microscope objective lens heater (TOKAI HIT) and was monitored by using a thermocouple (TSU-0125 thermometer with a TSU-7225 probe, TOKAI HIT). A Femtojet (Eppendorf) controlled by a micromanipulator (Eppendorf) was used for microinjection. The fluorescent nanogel thermometer was dissolved in an aqueous solution (1 w/v %) containing 80 mM KCl, 10 mM K_2HPO_4, and 4 mM NaCl. The solution was filtered using an Ultrafree-MC centrifugal filter (Millipore) and microinjected into the cytoplasm with a glass capillary needle, Femtotips II (Eppendorf). The volume of the injected solution was estimated to be 2 fL.

Live cell imaging was performed with an IX70 inverted microscope (Olympus) equipped with an objective lens (UplanApo 60x/1.40 NA PH3 NA, Olympus). A cooled CCD camera (ORCA-ER, Hamamatsu Photonics) was used to acquire cell images. Fluorescence images were obtained with a sapphire laser (Model 488–30 CDRH, Coherent), a DM505 dichroic mirror (Olympus), and a BA515–550 emission filter (Olympus). The photodecomposition of the DBThD nanogels inside the COS7 cells was examined under continuous photoirradiation by the sapphire laser (Model 488–30 CDRH). The images obtained were quantitatively analyzed with AQUA-Lite ver. 10 (Hamamatsu Photonics).

Acknowledgements

S.U. and N.I. thank the Japan Science and Technology Agency (JST) for financial support from the Development of Advanced Measurement and Analysis Systems program.

[1] G. Weber, F. J. Farris, *Biochemistry* **1979**, *18*, 3075–3078.
[2] a) D. J. R. Laurence, *Biochem. J.* **1954**, *56*, xxxi; b) L. Stryer, *J. Mol. Biol.* **1965**, *13*, 482–495; c) S.-C. Tu, J. W. Hastings, *Biochemistry* **1975**, *14*, 4310–4316.
[3] Y.-H. Li, L.-M. Chan, L. Tyer, R. T. Moody, C. M. Himel, D. M. Hercules, *J. Am. Chem. Soc.* **1975**, *97*, 3118–3126.
[4] a) S. Fery-Forgues, J.-P. Fayet, A. Lopez, *J. Photochem. Photobiol. A* **1993**, *70*, 229–243; b) S. Uchiyama, T. Santa, K. Imai, *J. Chem. Soc. Perkin Trans. 2* **1999**, 2525–2532.
[5] a) D. L. Sackett, J. Wolff, *Anal. Biochem.* **1987**, *167*, 228–234; b) A. Cser, K. Nagy, L. Biczók, *Chem. Phys. Lett.* **2002**, *360*, 473–478.
[6] a) K. Kalyanasundaram, J. K. Thomas, *J. Am. Chem. Soc.* **1977**, *99*, 2039–2044; b) K. Kalyanasundaram, J. K. Thomas, *J. Phys. Chem.* **1977**, *81*, 2176–2180; c) J. S. Seixas de Melo, R. S. Becker, A. L. Maçanita, *J. Phys. Chem.* **1994**, *98*, 6054–6058; d) S. Uchiyama, K. Takehira, T. Yoshihara, S. Tobita, T. Ohwada, *Org. Lett.* **2006**, *8*, 5869–5872; e) C. Toro, A. Thibert, L. De Boni, A. E. Masunov, F. E. Hernández, *J. Phys. Chem. B* **2008**, *112*, 929–937.
[7] a) G. M. Edelman, W. O. McClure, *Acc. Chem. Res.* **1968**, *1*, 65–70; b) R. B. Macgregor, G. Weber, *Nature* **1986**, *319*, 70–73; c) B. E. Cohen, T. B. McAnaney, E. S. Park, Y. N. Jan, S. G. Boxer, L. Y. Jan, *Science* **2002**, *296*, 1700–1703.
[8] A. Okamoto, K. Tainaka, I. Saito, *Bioconjugate Chem.* **2005**, *16*, 1105–1111.
[9] a) N. Kitamura, N. Sakata, H.-B. Kim, S. Habuchi, *Anal. Sci.* **1999**, *15*, 413–419; b) K. Nagy, S. Göktürk, L. Biczók, *J. Phys. Chem. A* **2003**, *107*, 8784–8790.
[10] E. Carlier, A. Revillon, A. Guyot, J.-P. Chauvet, *Eur. Polym. J.* **1993**, *29*, 819–823.
[11] S. Chen, X. Li, H. Ma, *ChemBioChem* **2009**, *10*, 1200–1207.
[12] B. E. Cohen, A. Pralle, X. Yao, G. Swaminath, C. S. Gandhi, Y. N. Jan, B. K. Kobilka, E. Y. Isacoff, L. Y. Jan, *Proc. Natl. Acad. Sci. USA* **2005**, *102*, 965–970.
[13] J. R. Simard, S. Klüter, C. Grütter, M. Getlik, M. Rabiller, H. B. Rode, D. Rauh, *Nat. Chem. Biol.* **2009**, *5*, 394–396.
[14] a) J. S. Mills, M. P. Walsh, K. Nemcek, J. D. Johnson, *Biochemistry* **1988**, *27*, 991–996; b) D. J. Sloan, H. W. Hellinga, *Protein Eng.* **1998**, *11*, 819–823.
[15] a) M. E. Vázquez, D. M. Rothman, B. Imperiali, *Org. Biomol. Chem.* **2004**, *2*, 1965–1966; b) M. E. Vázquez, J. B. Blanco, B. Imperiali, *J. Am. Chem. Soc.* **2005**, *127*, 1300–1306; c) P. Venkatraman, T. T. Nguyen, M. Sainlos, O. Bilsel, S. Chitta, B. Imperiali, L. J. Stern, *Nat. Chem. Biol.* **2007**, *3*, 222–228; d) M. Sainlos, W. S. Iskenderian, B. Imperiali, *J. Am. Chem. Soc.* **2009**, *131*, 6680–6682; e) E. Pazos, M. Pérez, H. Gutiérrez-de-Terán, M. Orzáez, T. Guevara, J. L. Mascareñas, M. E. Vázquez, *Org. Biomol. Chem.* **2011**, *9*, 7629–7632.
[16] A. H. Nguyen, V. T. Nguyen, Y. Kamio, H. Higuchi, *Biochemistry* **2006**, *45*, 2570–2576.
[17] For a review, see: G. S. Loving, M. Sainlos, B. Imperiali, *Trends Biotechnol.* **2010**, *28*, 73–83.
[18] For reviews, see: a) H. W. Hellinga, J. S. Marvin, *Trends Biotechnol.* **1998**, *16*, 183–189; b) E. Pazos, O. Vázquez, J. L. Mascareñas, M. E. Vázquez, *Chem. Soc. Rev.* **2009**, *38*, 3348–3359.

[19] For reviews, see: a) J. Hu, S. Liu, *Macromolecules* **2010**, *43*, 8315–8330; b) C. Pietsch, U. S. Schubert, R. Hoogenboom, *Chem. Commun.* **2011**, *47*, 8750–8765.
[20] C. Pietsch, R. Hoogenboom, U. S. Schubert, *Polym. Chem.* **2010**, *1*, 1005–1008.
[21] G. K. Walkup, B. Imperiali, *J. Am. Chem. Soc.* **1996**, *118*, 3053–3054.
[22] a) R. L. Kincaid, M. Vaughan, J. C. Osborne Jr., V. A. Tkachuk, *J. Biol. Chem.* **1982**, *257*, 10638–10643; b) V. Schauer-Vukasinovic, L. Cullen, S. Daunert, *J. Am. Chem. Soc.* **1997**, *119*, 11102–11103.
[23] A. Torrado, G. K. Walkup, B. Imperiali, *J. Am. Chem. Soc.* **1998**, *120*, 609–610.
[24] S. Deo, H. A. Godwin, *J. Am. Chem. Soc.* **2000**, *122*, 174–175.
[25] S. Shrestha, L. L. E. Salins, C. M. Ensor, S. Daunert, *Biotechnol. Bioeng.* **2002**, *78*, 517–526.
[26] L. L. E. Salins, S. K. Deo, S. Daunert, *Sens. Actuators B* **2004**, *97*, 81–89.
[27] J. S. Marvin, H. W. Hellinga, *J. Am. Chem. Soc.* **1998**, *120*, 7–11.
[28] a) L. Q. Zhou, A. E. G. Cass, *Biosens. Bioelectron.* **1991**, *6*, 445–450; b) G. Gilardi, L. Q. Zhou, L. Hibbert, A. E. G. Cass, *Anal. Chem.* **1994**, *66*, 3840–3847.
[29] a) J. D. Dattelbaum, J. R. Lakowicz, *Anal. Biochem.* **2001**, *291*, 89–95; b) A. Wada, M. Mie, M. Aizawa, P. Lahoud, A. E. G. Cass, E. Kobatake, *J. Am. Chem. Soc.* **2003**, *125*, 16228–16234.
[30] a) S. P. Gilbert, M. R. Webb, M. Brune, K. A. Johnson, *Nature* **1995**, *373*, 671–676; b) C. Lionne, M. Brune, M. R. Webb, F. Travers, T. Barman, *FEBS Lett.* **1995**, *364*, 59–62; c) A. E. Nixon, M. Brune, P. N. Lowe, M. R. Webb, *Biochemistry* **1995**, *34*, 15592–15598; d) Z.-H. He, R. K. Chillingworth, M. Brune, J. E. T. Corrie, D. R. Trentham, M. R. Webb, M. A. Ferenczi, *J. Physiol.* **1997**, *501*, 125–148.
[31] a) S. Uchiyama, T. Santa, N. Okiyama, T. Fukushima, K. Imai, *Biomed. Chromatogr.* **2001**, *15*, 295–318; b) T. Santa, T. Fukushima, T. Ichibangase, K. Imai, *Biomed. Chromatogr.* **2008**, *22*, 343–353.
[32] C. Gota, S. Uchiyama, T. Yoshihara, S. Tobita, T. Ohwada, *J. Phys. Chem. B* **2008**, *112*, 2829–2836.
[33] a) S. Uchiyama, Y. Matsumura, A. P. de Silva, K. Iwai, *Anal. Chem.* **2003**, *75*, 5926–5935; b) S. Uchiyama, Y. Matsumura, A. P. de Silva, K. Iwai, *Anal. Chem.* **2004**, *76*, 1793–1798; c) S. Uchiyama, N. Kawai, A. P. de Silva, K. Iwai, *J. Am. Chem. Soc.* **2004**, *126*, 3032–3033; d) C. Gota, S. Uchiyama, T. Ohwada, *Analyst* **2007**, *132*, 121–126.
[34] C. Gota, K. Okabe, T. Funatsu, Y. Harada, S. Uchiyama, *J. Am. Chem. Soc.* **2009**, *131*, 2766–2767.
[35] S. E. Braslavsky, G. E. Heibel, *Chem. Rev.* **1992**, *92*, 1381–1410.
[36] For corresponding changes in the fluorescence spectra of DBThD-IA, DBSeD-IA, and DBD-IA, see Figure S9 in the Supporting Information.
[37] S. Uchiyama, K. Takehira, S. Kohtani, T. Santa, R. Nakagaki, S. Tobita, K. Imai, *Phys. Chem. Chem. Phys.* **2002**, *4*, 4514–4522.
[38] It was also determined that the quantum yield for the photodecomposition of NBD-NHMe is 2.0×10^{-3} in acetonitrile.
[39] a) S. Lamansky, P. Djurovich, D. Murphys, F. Abdel-Razzaq, H.-E. Lee, C. Adachi, P. E. Burrows, S. R. Forrest, M. E. Thompson, *J. Am. Chem. Soc.* **2001**, *123*, 4304–4312; b) S. Zhang, M. Hosaka, T. Yoshihara, K. Negishi, Y. Iida, S. Tobita, T. Takeuchi, *Cancer Res.* **2010**, *70*, 4490–4498.
[40] We found a remarkable temperature shift (ca. 3 °C) of the response curve when the temperature-dependent parameter was changed from fluorescence intensity to fluorescence lifetime. The reason for this shift is unclear, but it is thought to occur because the fluorescence lifetime of the DBThD-IA units in the DBThD nanogels is mainly affected by hydrogen bonding, whereas their fluorescence intensity varies predominantly as a result of a change in the polarity of the environment.
[41] B. Valuer, *Molecular Fluorescence*, Wiley-VCH, Weinheim, **2001**, pp. 206.
[42] The increases in the dipole moment arising from the excitation are supported by the relationship between the Stokes shift and the solvent polarity parameter, see Figure S10 in the Supporting Information and also: a) C. Reichardt, *Chem. Rev.* **1994**, *94*, 2319–2358; b) M. Ravi, T. Soujanya, A. Samanta, T. P. Radhakrishnan, *J. Chem. Soc. Faraday Trans.* **1995**, *91*, 2739–2742; c) R. W. Sinkeldam, Y. Tor, *Org. Biomol. Chem.* **2007**, *5*, 2523–2528.
[43] a) N. J. Turro, V. Ramamurthy, J. C. Scaiano, *Modern Molecular Photochemistry of Organic Molecules*, University Science Books, Sausalito, **2010**; pp. 303–304; b) R. Englman, J. Jortner, *Mol. Phys.* **1970**, *18*, 145–164; c) J. V. Caspar, B. P. Sullivan, E. M. Kober, T. J. Meyer, *Chem. Phys. Lett.* **1982**, *91*, 91–95.
[44] a) H. Inoue, M. Hida, N. Nakashima, K. Yoshihara, *J. Phys. Chem.* **1982**, *86*, 3184–3188; b) T. Yatsuhashi, H. Inoue, *J. Phys. Chem. A* **1997**, *101*, 8166–8173; c) T. Yoshihara, H. Shimada, H. Shizuka, S. Tobita, *Phys. Chem. Chem. Phys.* **2001**, *3*, 4972–4978.
[45] E. Sawicki, A. Carr, *J. Org. Chem.* **1957**, *22*, 503–506.
[46] T. Y. Ohulchanskyy, D. J. Donnelly, M. R. Detty, P. N. Prasad, *J. Phys. Chem. B* **2004**, *108*, 8668–8672.
[47] H. Saimaru, M. Masuda, C. Toriumi, T. Santa, E. Ichikawa, N. Takamura, K. Imai, *J. Mater. Chem.* **2005**, *15*, 2865–2872.
[48] G. G. Aloisi, F. Elisei, S. Moro, G. Miolo, F. Dall′Acqua, *Photochem. Photobiol.* **2000**, *71*, 506–513.
[49] M. Montalti, A. Credi, L. Prodi, M. T. Gandolfi, *Handbook of Photochemistry 3rd ed.*, CRC Press, Boca Raton, **2006**.
[50] T. Mukai, M. Nitta, *J. Chem. Soc. D: Chem. Commun.* **1970**, 1192.
[51] A. Mori, Y. Mikami, H. Saito, K. Kobayashi, S. Miyairi, H. Ohshima, T. Takabatake, *Heterocycles* **2011**, *83*, 619–625.
[52] T. S. Cantrell, W. S. Haller, *Chem. Commun. (London)* **1968**, 977–978.
[53] S. Uchiyama, A. P. de Silva, K. Iwai, *J. Chem. Educ.* **2006**, *83*, 720–727.
[54] K. Iwai, Y. Matsumura, S. Uchiyama, A. P. de Silva, *J. Mater. Chem.* **2005**, *15*, 2796–2800.
[55] a) Y. Shiraishi, R. Miyamoto, X. Zhang, T. Hirai, *Org. Lett.* **2007**, *9*, 3921–3924; b) Y. Shiraishi, R. Miyamoto, T. Hirai, *J. Photochem. Photobiol. A* **2008**, *200*, 432–437.
[56] Y. Shiraishi, R. Miyamoto, T. Hirai, *Langmuir* **2008**, *24*, 4273–4279.
[57] C. P. Mpamhanga, D. Spinks, L. B. Tulloch, E. J. Shanks, D. A. Robinson, I. T. Collie, A. H. Fairlamb, P. G. Wyatt, J. A. Frearson, W. N. Hunter, I. H. Gilbert, R. Brenk, *J. Med. Chem.* **2009**, *52*, 4454–4465.
[58] C. W. Bird, G. W. H. Cheeseman, A. A. Sarsfield, *J. Chem. Soc.* **1963**, 4767–4770.
[59] J. W. Eastman, *Photochem. Photobiol.* **1967**, *6*, 55–72.
[60] M. Fischer, J. Georges, *Chem. Phys. Lett.* **1996**, *260*, 115–118.
[61] J. Yguerabide, *Rev. Sci. Instrum.* **1968**, *39*, 1048–1052.
[62] M. J. Kamlet, J.-L. M. Abboud, M. H. Abraham, R. W. Taft, *J. Org. Chem.* **1983**, *48*, 2877–2887.
[63] D. W. Davidson, *Can. J. Chem.* **1957**, *35*, 458–473.
[64] J. Wyman Jr., E. N. Ingalls, *J. Am. Chem. Soc.* **1938**, *60*, 1182–1184.

Received: February 23, 2012
Published online: July 3, 2012

